Hidden Cores of Active Galactic Nuclei as the Origin of Medium-Energy Neutrinos: Critical Tests with the MeV Gamma-Ray Connection

Kohta Murase[1,2,3,4] Shigeo S. Kimura[1,2,3] and Peter Mészáros[1,2,3]

[1]*Department of Physics, The Pennsylvania State University, University Park, Pennsylvania 16802, USA*
[2]*Department of Astronomy & Astrophysics, The Pennsylvania State University, University Park, Pennsylvania 16802, USA*
[3]*Center for Multimessenger Astrophysics, Institute for Gravitation and the Cosmos,*
The Pennsylvania State University, University Park, Pennsylvania 16802, USA
[4]*Yukawa Institute for Theoretical Physics, Kyoto, Kyoto 606-8502 Japan*

Mysteries about the origin of high-energy cosmic neutrinos have deepened by the recent IceCube measurement of a large diffuse flux in the 10–100 TeV range. Based on the standard disk-corona picture of active galactic nuclei (AGN), we present a phenomenological model enabling us to systematically calculate the spectral sequence of multimessenger emission from the AGN coronae. We show that protons in the coronal plasma can be stochastically accelerated up to PeV energies by plasma turbulence, and find that the model explains the large diffuse flux of medium-energy neutrinos if the cosmic rays carry only a few percent of the thermal energy. We find that the Bethe-Heitler process plays a crucial role in connecting these neutrinos and cascaded MeV gamma rays, and point out that the gamma-ray flux can even be enhanced by the reacceleration of secondary pairs. Critical tests of the model are given by its prediction that a significant fraction of the MeV gamma-ray background correlates with ∼10 TeV neutrinos, and nearby Seyfert galaxies including NGC 1068 are promising targets for IceCube, KM3Net, IceCube-Gen2, and future MeV gamma-ray telescopes.

The origin of cosmic neutrinos observed in IceCube is a major enigma [1,2], and the latest data of high- and medium-energy starting events and shower events [3–5] are more puzzling. The atmospheric background of high-energy electron neutrinos is lower than that of muon neutrinos, allowing us to analyze the data below 100 TeV [6,7]. The extragalactic neutrino background (ENB) at these energies has shown a larger flux with a softer spectrum, compared to the ≳100 TeV data [8,9]. The comparison with the extragalactic gamma-ray background (EGB) measured by *Fermi* indicates that the 10–100 TeV ENB originates from *hidden* sources preventing the escape of GeV–TeV gamma rays [10].

Active galactic nuclei (AGN) are major contributors to the energetics of high-energy cosmic radiations [11]; radio quiet (RQ) AGN are dominant in the extragalactic x-ray sky [12–16], and jetted AGN that are typically radio loud (RL) dominantly explain the EGB [17–19]. AGN may also explain the MeV gamma-ray background whose origin has been under debate (e.g., Refs. [20–22]).

High-energy neutrino production in the vicinity of supermassive black holes (SMBHs) were discussed early on [23–26], in particular to explain x-ray emission by cosmic-ray (CR) induced cascades assuming the existence of high Mach number accretion shocks at the inner edge of the disk [26–29]. However, cutoff features evident in the x-ray spectra of Seyfert galaxies and the absence of

electron-positron annihilation lines ruled out the simple cascade scenario for the x-ray origin (e.g., Refs. [30,31]). In the standard disk-corona scenario, the observed x rays are attributed to thermal Comptonization of disk photons [32–36], and electrons are presumably heated in the coronal region [37,38]. There has been significant progress in our understanding of accretion disks with the identification of the magnetorotational instability (MRI) [39,40], which can result in the formation of a corona above the disk as a direct consequence of the accretion dynamics and magnetic dissipation (e.g., Refs. [41–47]).

Accompanied turbulence and magnetic reconnections are important for particle acceleration [48]. The roles of nonthermal particles have been studied in the context of radiatively inefficient accretion flows (RIAFs) [49,50], in which the plasma is often collisionless because Coulomb collisions are negligible for protons (e.g., Refs. [51–56]). Recent studies based on numerical simulations of the MRI [57,58] support the idea that high-energy ions may be accelerated in the presence of the magnetohydrodynamic (MHD) turbulence.

The vicinity of SMBHs is often optically thick to GeV–TeV gamma rays, so that CR acceleration [59] cannot be directly probed by these photons, but high-energy neutrinos can be used as a unique probe of the physics of AGN cores. In this work, we present a new concrete model for these high-energy emissions (see Fig. 1). Spectral energy
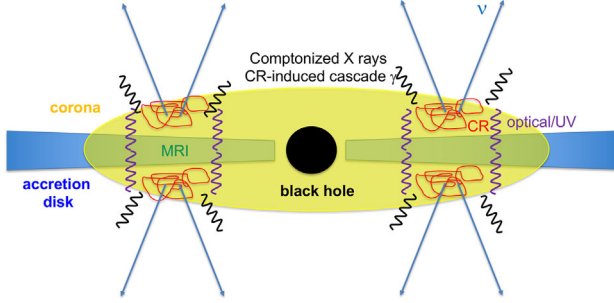
FIG. 1. Schematic picture of the AGN disk-corona scenario. Protons are accelerated by plasma turbulence generated in the coronae, and produce high-energy neutrinos and cascaded gamma rays via interactions with matter and radiation.

FIG. 2. Disk-corona SEDs used in this work, for $L_X = 10^{42}$, 10^{43}, 10^{44}, 10^{45}, and 10^{46} erg s^{-1} (from bottom to top). See text for details.

distributions (SEDs) are constructed from the data and from empirical relations, and then we compute neutrino and cascade gamma-ray spectra by consistently solving particle transport equations. We demonstrate the importance of future MeV gamma-ray observations for revealing the origin of IceCube neutrinos especially in the medium-energy ($\sim$10–100 TeV) range and for testing neutrino emission from NGC 1068 and other AGN.

We use a notation with $Q_x = Q \times 10^x$ in CGS units.

Phenomenological prescription of AGN disk coronae.— We begin by providing a phenomenological disk-corona model based on the existing data. Multiwavelength SEDs of Seyfert galaxies have been extensively studied, consisting of several components; radio emission (see Ref. [60]), infrared emission from a dust torus [61], optical and ultraviolet components from an accretion disk [62], and x rays from a corona [33]. The latter two components are relevant for this work.

The "blue" bump, which has been seen in many AGN, is attributed to multitemperature blackbody emission from a geometrically thin, optically thick disk [63]. The averaged SEDs are provided in Ref. [64] as a function of the Eddington ratio, $\lambda_{\rm Edd} = L_{\rm bol}/L_{\rm Edd}$, where $L_{\rm bol}$ and $L_{\rm Edd} \approx 1.26 \times 10^{45}$ erg s^{-1} $(M/10^7 M_\odot)$ are bolometric and Eddington luminosities, respectively, and M is the SMBH mass. The disk component is expected to have a cutoff in the ultraviolet range. Hot thermal electrons in a corona, with an electron temperature of $T_e \sim 10^9$ K, energize the disk photons by Compton upscattering. The consequent x-ray spectrum can be described by a power law with an exponential cutoff, in which the photon index (Γ_X) and the cutoff energy ($\varepsilon_{X,\rm cut}$) can also be estimated from $\lambda_{\rm Edd}$ [31,65]. Observations have revealed the relationship between the x-ray luminosity L_X and $L_{\rm bol}$ [66] [where one typically sees $L_X \sim (0.01 - 0.1)L_{\rm bol}$], by which the disk-corona SEDs can be modeled as a function of L_X and M. In this work, we consider contributions from AGN with the typical SMBH mass for a given L_X, using $M \approx 2.0 \times 10^7 M_\odot (L_X/1.16 \times 10^{43}$ erg s$^{-1})^{0.746}$ [67]. The resulting disk-corona SED templates in our model are shown in
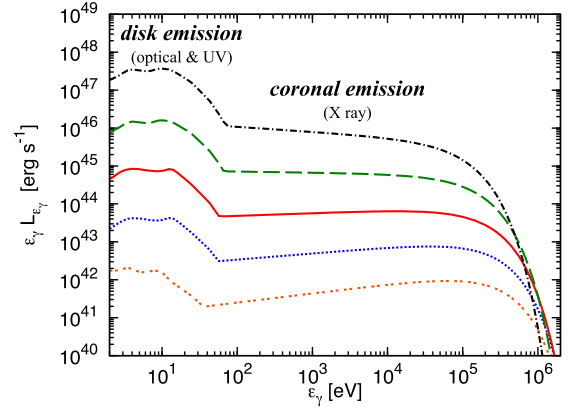
Fig. 2 (see Supplemental Material [68] for details), which enables us to quantitatively evaluate CR, neutrino and cascade gamma-ray emission.

Next we estimate the nucleon density n_p and coronal magnetic field strength B. Let us consider a corona with the radius $R \equiv \mathcal{R}R_S$ and the scale height H, where $\mathcal{R}$ is the normalized coronal radius and $R_S = 2GM/c^2$ is the Schwarzschild radius. Then the nucleon density is expressed by $n_p \approx \tau_T/(\sigma_T H)$, where τ_T is the Thomson optical depth that is typically $\sim$0.1–1. The standard accretion theory [69,70] gives the coronal scale height $H \approx (C_s/V_K)\mathcal{R}R_S = \mathcal{R}R_S/\sqrt{3}$, where $C_s = \sqrt{k_B T_p/m_p} = c/\sqrt{6\mathcal{R}}$ is the sound velocity, and $V_K = \sqrt{GM/R} = c/\sqrt{2\mathcal{R}}$ is the Keplerian velocity. For an optically thin corona, the electron temperature is estimated by $T_e \approx \varepsilon_{X,\rm cut}/(2k_B)$, and τ_T is empirically determined from Γ_X and $k_B T_e$ [31]. We expect that thermal protons are at the virial temperature $T_p = GMm_p/(3\mathcal{R}R_S k_B) = m_p c^2/(6\mathcal{R}k_B)$, implying that the corona may be characterized by two temperatures, i.e., $T_p > T_e$ [71,72]. Finally, the magnetic field is given by $B = \sqrt{8\pi n_p k_B T_p/\beta}$ with plasma beta (β).

Many physical quantities (including the SEDs) can be estimated observationally and empirically. Thus, for a given L_X, parameters characterizing the corona ($\mathcal{R}$, β, α) are remaining. They are also constrained in a certain range by observations [73,74] and numerical simulations [45,47]. For example, recent MHD simulations show that β in the coronae can be as low as 0.1–10 (e.g., Refs. [41,46]). We assume $\beta \lesssim 1$–3 and $\alpha = 0.1$ for the viscosity parameter [63], and adopt $\mathcal{R} = 30$.

Stochastic proton acceleration in coronae.—Standard AGN coronae are magnetized and turbulent, in which it is natural that protons are stochastically accelerated via plasma turbulence or magnetic reconnections. In this work, we solve the known Fokker-Planck equation that can describe the second order Fermi acceleration process

(e.g., Refs. [75–78]). Here we describe key points in the calculations of CR spectra (see Supplemental Material [68] or an accompanying paper [79] for technical details). The stochastic acceleration time is given by $t_{acc} \approx \eta(c/V_A)^2(H/c)(\varepsilon_p/eBH)^{2-q}$, where V_A is the Alfvén velocity and η is the inverse of the turbulence strength [80,81]. We consider $q \sim 3/2 - 5/3$, which is not inconsistent with the recent simulations [58], together with $\eta \sim 10$. The stochastic acceleration process is typically slower than the first order Fermi acceleration, which competes with cooling and escape processes. We find that for luminous AGN the Bethe-Heitler pair production $(p\gamma \rightarrow pe^+e^-)$ is the most important cooling process because of copious disk photons, which determines the proton maximum energy. For our model parameters, the CR spectrum has a cutoff at $\varepsilon_p \sim 0.1–1$ PeV, leading to a cutoff at $\varepsilon_\nu \sim 5–50$ TeV in the neutrino spectrum. Note that all the loss timescales can uniquely be evaluated within our disk-corona model, and this result is only sensitive to η and q for a given set of coronal parameters. Although the resulting CR spectra (that are known to be hard) are numerically obtained in this work, we stress that spectra of $p\gamma$ neutrinos are independently predicted to be hard, because the photomeson production occurs only for protons whose energies exceed the pion production threshold [10,79]. The CR pressure to explain the neutrino data turns out to be $\sim(1 - 10)\%$ of the thermal pressure, by which the normalization of CRs is set.

For coronae considered here, the infall and dissipation times are $t_{fall} \simeq 2.5 \times 10^6$ s $\alpha_{-1}^{-1}(\mathcal{R}/30)^{3/2}R_{S,13.5}$ and $t_{diss} \simeq 1.7 \times 10^5$ s $(\mathcal{R}/30)^{3/2}R_{S,13.5}\beta^{1/2}$, respectively. The Coulomb relaxation timescales for protons [e.g., $t_{C,pe} \sim 4 \times 10^5s(\mathcal{R}/30)R_{S,13.5}(\tau_T/0.5)^{-1}(k_BT_e/0.1\text{MeV})^{3/2}$] are longer than t_{diss} (especially for $\beta \lesssim 1$), so turbulent acceleration may operate for protons rather than electrons (and acceleration by small-scale magnetic reconnections may occur [82,83]). This justifies our assumption on CR acceleration (cf. Refs. [79,84–86] for RIAFs).

Connection between 10–100 TeV neutrinos and MeV gamma rays.—Accelerated CR protons interact with matter and radiation modeled in the previous section, producing secondary particles. We compute neutrino and gamma-ray spectra as a function of L_X, by utilizing the code to solve kinetic equations with electromagnetic cascades taken into account [87,88]. Secondary injections by the Bethe-Heitler and $p\gamma$ processes are approximately treated as $\varepsilon_e^2(d\dot{N}_e^{BH}/d\varepsilon_e)|_{\varepsilon_e=(m_e/m_p)\varepsilon_p} \approx t_{BH}^{-1}\varepsilon_p^2(dN_{CR}/d\varepsilon_p)$ [89–91], $\varepsilon_e^2(d\dot{N}_e^{p\gamma}/d\varepsilon_e)|_{\varepsilon_e=0.05\varepsilon_p} \approx (1/3)\varepsilon_\nu^2(d\dot{N}_\nu^{p\gamma}/d\varepsilon_\nu)|_{\varepsilon_\nu=0.05\varepsilon_p} \approx (1/8)t_{p\gamma}^{-1}\varepsilon_p^2(dN_{CR}/d\varepsilon_p)$, and $\varepsilon_\gamma^2(d\dot{N}_\gamma^{p\gamma}/d\varepsilon_\gamma)|_{\varepsilon_\gamma=0.1\varepsilon_p} \approx (1/2)t_{p\gamma}^{-1}\varepsilon_p^2(dN_{CR}/d\varepsilon_p)$. The cascade photon spectra are broad, being determined by the energy reprocessing via two-photon annihilation, synchrotron radiation, and inverse Compton emission.

The EGB and ENB are numerically calculated via the line-of-sight integral with the convolution of the x-ray luminosity function given by Ref. [16] (see also Supplemental Material [68], which includes Refs. [92–99]). Note that the luminosity density of AGN evolves as redshift z, with a peak around $z \sim 1–2$, and our prescription enables us to *simultaneously* predict the x-ray background, EGB and ENB. The results are shown in Fig. 3, and our AGN corona model can explain the ENB at ~ 30 TeV energies with a steep spectrum at higher energies (due to different proton maximum energies), possibly simultaneously with the MeV EGB. We find that the required CR pressure (P_{CR}) is only $\sim 1\%$ of the thermal pressure (P_{th}), so the energetics requirement is not demanding in our AGN corona model (see Supplemental Material [68]).

Remarkably, we find that high-energy neutrinos are produced by *both* pp and $p\gamma$ interactions. The disk-corona model indicates $\tau_T \approx n_p\sigma_T\mathcal{R}R_S/\sqrt{3} \sim 0.1–1$, leading to the effective pp optical depth

$$f_{pp} \approx t_{esc}/t_{pp} \approx n_p(\kappa_{pp}\sigma_{pp})R(c/V_{fall})$$
$$\sim 2(\tau_T/0.5)\alpha_{-1}^{-1}(\mathcal{R}/30)^{1/2}, \tag{1}$$

where $\sigma_{pp} \sim 4 \times 10^{-26}$ cm^2 is the pp cross section, $\kappa_{pp} \sim 0.5$ is the proton inelasticity, and $V_{fall} = \alpha V_K$ is the infall velocity. Coronal x rays provide target photons for the photomeson production, whose effective optical depth [10,104] for $\tau_T \lesssim 1$ is

$$f_{p\gamma} \approx t_{esc}/t_{p\gamma} \approx \eta_{p\gamma}\hat{\sigma}_{p\gamma}R(c/V_{fall})n_X(\varepsilon_p/\tilde{\varepsilon}_{p\gamma-X})^{\Gamma_X-1}$$
$$\sim 2\frac{\eta_{p\gamma}L_{X,44}(\varepsilon_p/\tilde{\varepsilon}_{p\gamma-X})^{\Gamma_X-1}}{\alpha_{-1}(\mathcal{R}/30)^{1/2}R_{S,13.5}(\varepsilon_X/1\text{ keV})}, \tag{2}$$
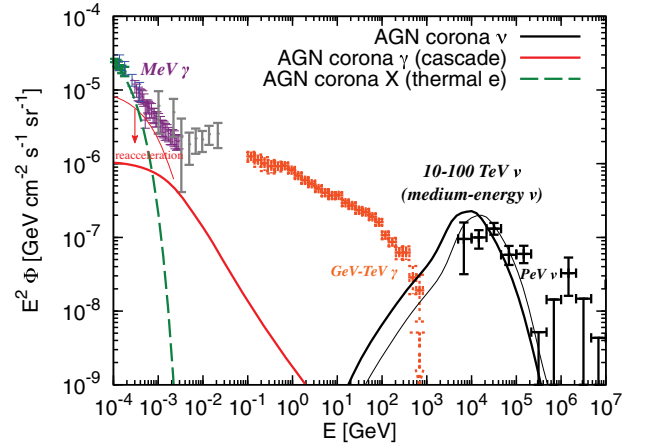
FIG. 3. EGB and ENB spectra in our AGN corona model. The data are taken from *Swift* BAT [15] (green), Nagoya balloon [100] (blue), SMM [101] (purple), COMPTEL [102] (gray), *Fermi* LAT [103] (orange), and IceCube shower events (black) [5] (consistent with the global fit [4]). Solid thick (thin) curves are for $\beta = 1$ and $q = 5/3$ ($\beta = 3$ and $q = 3/2$ with the reacceleration contribution), respectively.

where $\eta_{p\gamma} \approx 2/(1+\Gamma_X)$, $\hat{\sigma}_{p\gamma} \sim 0.7 \times 10^{-28}$ cm^2 is the attenuation $p\gamma$ cross section, $\bar{\varepsilon}_\Delta \sim 0.3$ GeV, $\tilde{\varepsilon}_{p\gamma-X} = 0.5 m_p c^2 \bar{\varepsilon}_\Delta/\varepsilon_X \simeq 0.14$ PeV$(\varepsilon_X/1$ keV$)^{-1}$, and $n_X \sim L_X/(2\pi R^2 c\varepsilon_X)$ is used. The total meson production optical depth is given by $f_{\mathrm{mes}} = f_{p\gamma} + f_{pp}$, which always exceeds unity in our model. Note that the spectrum of $p\gamma$ neutrinos should be hard at low energies, because only sufficiently high-energy protons can produce pions via $p\gamma$ interactions with x-ray photons.

Note that $\sim$10–100 TeV neutrinos originate from $\sim$0.2–2 PeV CRs. Unlike in previous studies explaining the IceCube data [105,106], here in fact the disk photons are not much relevant for the photomeson production because its threshold energy is $\tilde{\varepsilon}_{p\gamma\text{-th}} \simeq 3.4$ PeV$(\varepsilon_{\mathrm{disk}}/10$ eV$)^{-1}$. Rather, CR protons responsible for the medium-energy neutrinos should efficiently interact via the Bethe-Heitler process because the characteristic energy is $\tilde{\varepsilon}_{\mathrm{BH}\text{-disk}} \approx 0.5 m_p c^2 \bar{\varepsilon}_{\mathrm{BH}}/\varepsilon_{\mathrm{disk}} \simeq 0.47$ PeV$(\varepsilon_{\mathrm{disk}}/10$ eV$)^{-1}$, where $\bar{\varepsilon}_{\mathrm{BH}} \sim 10(2m_e c^2) \sim 10$ MeV [89–91]. With the disk photon density $n_{\mathrm{disk}} \sim L_{\mathrm{disk}}/(2\pi R^2 c\varepsilon_{\mathrm{disk}})$ for $\tau_T \lesssim 1$, the effective Bethe-Heitler optical depth (with $\hat{\sigma}_{\mathrm{BH}} \sim 0.8 \times 10^{-30}$ cm^2) is

$$f_{\mathrm{BH}} \approx n_{\mathrm{disk}}\hat{\sigma}_{\mathrm{BH}}R(c/V_{\mathrm{fall}})$$
$$\sim 40 L_{\mathrm{disk},45.3}\alpha_{-1}^{-1}(\mathcal{R}/30)^{-1/2}R_{S,13.5}^{-1}(10\text{ eV}/\varepsilon_{\mathrm{disk}}), \quad (3)$$

which is much larger than $f_{p\gamma}$. The dominance of the Bethe-Heitler cooling is a direct consequence of the observed disk-corona SEDs. The 10–100 TeV neutrino flux is suppressed by $\sim f_{\mathrm{mes}}/f_{\mathrm{BH}}$, predicting the tight relationship with the MeV gamma-ray flux.

Analytically, the medium-energy ENB flux is given by

$$E_\nu^2\Phi_\nu \sim 10^{-7}\text{ GeVcm}^{-2}\text{s}^{-1}\text{sr}^{-1}\left(\frac{2K}{1+K}\right)\mathcal{R}_p^{-1}\left(\frac{\xi_z}{3}\right)$$
$$\times\left(\frac{15f_{\mathrm{mes}}}{1+f_{\mathrm{BH}}+f_{\mathrm{mes}}}\right)\left(\frac{\xi_{\mathrm{CR},-1}L_X\rho_X}{2\times 10^{46}\text{ erg}\,\mathrm{Mpc}^{-3}\,\mathrm{yr}^{-1}}\right), \quad (4)$$

which is indeed consistent with the numerical results shown in Fig. 3. Here $K=1$ and $K=2$ for $p\gamma$ and pp interactions, respectively, $\xi_z \sim 3$ due to the redshift evolution of the AGN luminosity density [107,108], $\mathcal{R}_p$ is the conversion factor from bolometric to differential luminosities, and ξ_{CR} is the CR loading parameter defined against the x-ray luminosity, where $P_{\mathrm{CR}}/P_{\mathrm{th}} \sim 0.01$ corresponds to $\xi_{\mathrm{CR}} \sim 0.1$ in our model. The ENB and EGB are dominated by AGN with $L_X \sim 10^{44}\mathrm{ergs}^{-1}$ [16], for which the effective local number density is $\rho_X \sim 5 \times 10^{-6}\mathrm{Mpc}^{-3}$ [108].

The pp, $p\gamma$ and Bethe-Heitler processes all initiate cascades, whose emission appears in the MeV range. Thanks to the dominance of the Bethe-Heitler process, AGN responsible for the medium-energy ENB should contribute a large fraction $\gtrsim$10–30% of the MeV EGB.

When turbulent acceleration operates, the reacceleration of secondary pairs populated by cascades [109] can naturally enhance the gamma-ray flux. The critical energy of the pairs, $\varepsilon_{e,\mathrm{cl}}$, is determined by the balance between the acceleration time t_{acc} and the electron cooling time $t_{e\text{-cool}}$ (see Supplemental Material [68] and Refs. [109,110]). We find that the condition for the reacceleration is rather sensitive to B and t_{acc}. For example, with $\beta = 3$ and $q = 1.5$, the reaccelerated pairs can upscatter x-ray photons up to $\sim(\varepsilon_{e,\mathrm{cl}}/m_e c^2)^2\varepsilon_X \simeq 3.4$ MeV$(\varepsilon_{e,\mathrm{cl}}/30$ MeV$)^2(\varepsilon_X/1$ keV$)$, which may lead to the MeV gamma-ray tail. This possibility is demonstrated in Fig. 3, and the effective number fraction of reaccelerated pairs is constrained as $\lesssim$0.1%.

Multimessenger tests.—Our corona model robustly predicts $\sim$0.1–10 MeV gamma-ray emission in either a synchrotron or an inverse Compton cascade scenario, without any primary electron acceleration (see Fig. 4). A large flux of 10–100 TeV neutrinos should be accompanied by the injection of Bethe-Heitler pairs in the 100–300 GeV range (see Supplemental Material [68] for details) and form a fast cooling ε_e^{-2} spectrum down to MeV energies in the steady state. In the simple inverse Compton cascade scenario, the cascade spectrum is extended up to a break energy at $\sim$1–10 MeV, above which gamma rays are suppressed by $\gamma\gamma \to e^+e^-$. In reality, both synchrotron and inverse Compton processes can be important. The characteristic energy of synchrotron emission from Bethe-Heitler pairs is $\varepsilon_{\mathrm{syn}}^{\mathrm{BH}} \sim 1$ MeV $B_{2.5}(\varepsilon_p/0.5$ PeV$)^2$ [91]. Because disk photons lie in the $\sim$1–10 eV range, the Klein-Nishina effect is important for the Bethe-Heitler pairs. Synchrotron cascades occur if the photon
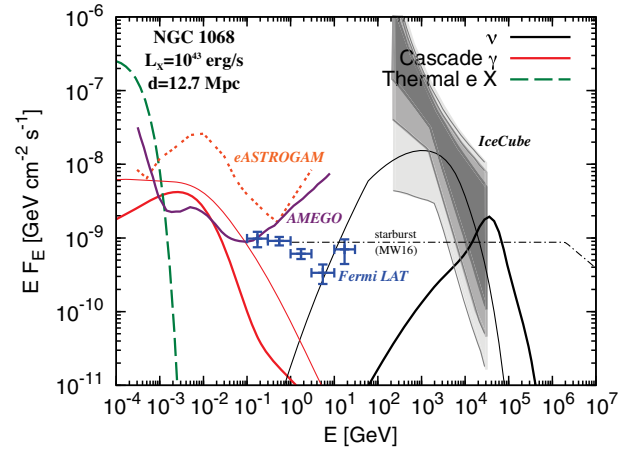
FIG. 4. Point source fluxes of all flavor neutrinos and gamma rays from a nearby AGN, NGC 1068. The ten-year IceCube data [111] and the *Fermi* gamma-ray data [112] are shown. For *eASTROGAM* [113] and *AMEGO* [114] sensitivities, the observation time of 10^6 s is assumed. Solid thick (thin) curves are for $\eta = 10$ and $P_{\mathrm{CR}}/P_{\mathrm{th}} = 0.7\%$ ($\eta = 70$ and $P_{\mathrm{CR}}/P_{\mathrm{th}} = 30\%$), respectively. For comparison, a neutrino flux in the starburst scenario of Murase and Waxman [108] is overlaid.

energy density is smaller than $\sim 10 B^2/(8\pi)$, i.e., $B \gtrsim 170~\mathrm{G}~L_{\mathrm{disk},45.3}^{1/2}(\mathcal{R}/30)^{-1} R_{S,13.5}^{-1}$.

The detectability of nearby Seyferts such as NGC 1068 and ESO 138-G001 is crucial for testing the model. MeV gamma-ray detection is promising with future telescopes like *eASTROGAM* [113], *GRAMS* [115], and *AMEGO* [114], e.g., *AMEGO*'s differential sensitivity suggests that point sources with $L_X \sim 10^{44}~\mathrm{erg~s}^{-1}$ are detectable up to $d \sim 70$–150 Mpc. At least a few of the brightest sources will be detected, and detections or nondetections of the MeV gamma-ray counterparts will support or falsify our corona model as the origin of ~ 30 TeV neutrinos. Interestingly, as demonstrated in Fig. 4, our corona model can explain the $\sim 3\sigma$ excess neutrino flux from NGC 1068 [111]. It also predicts that the x-ray brightest Seyferts (that are more in the southern sky) can be detected as neutrino point sources by IceCube-Gen2 and KM3Net (see also Supplemental Material [68], which includes Refs. [116–118]).

Summary and discussion.—We presented a new AGN corona model that can explain the medium-energy neutrino data. The observed disk-corona SEDs and known empirical relations enabled us to estimate model parameters, with which we solved particle transport equations and consistently computed subsequent electromagnetic cascades. Our coronal emission model provides clear, testable predictions relying on the neutrino–gamma-ray relationship that are largely independent of CR spectra. In particular, the dominance of the Bethe-Heitler pair production process is a direct consequence of the observed SEDs, leading to a natural connection with MeV gamma rays. Nearby Seyferts such as NGC 1068 and ESO 138-G001 will be promising targets for future MeV gamma-ray telescopes such as *eASTROGAM* and *AMEGO*. A good fraction of the MeV EGB may come from RQ AGN especially with secondary reacceleration, in which gamma-ray anisotropy searches should also be powerful [119]. Neutrino multiplet [108] and stacking searches with x-ray bright AGN are also promising, as encouraged by the latest neutrino source searches [111].

The proposed tests are crucial for unveiling nonthermal phenomena in the vicinity of SMBHs. In Seyferts and quasars, the plasma density is so high that a vacuum polar gap is diminished and GeV-TeV gamma rays are blocked. MeV gamma rays and neutrinos can escape and serve as a smoking gun of hidden CR acceleration that cannot be probed by x rays and lower-energy photons. Our results also strengthen the importance of further theoretical studies of disk-corona systems. Simulations on turbulent acceleration in coronae and particle-in-cell computations of magnetic reconnections are encouraged to understand the CR acceleration in such systems. Global MHD simulations will also be relevant to examine other speculative postulates such as accretion shocks [26,27,120,121] or colliding blobs [122], and to reveal the origin of low-frequency emission [123,124].

Note added.—Recently, we became aware of Ref. [125]. We thank Yoshiyuki Inoue for prior discussions. Both works are independent and complementary, but there are notable differences. First, we consistently calculated cosmic-ray and secondary neutrino and gamma-ray spectra based on the standard picture of magnetized coronae, rather than by hypothesized ``free-fall'' accretion shocks. The former picture is supported by recent simulations of the magnetorotational instability. Second, we focused on the mysterious origin of 10–100 TeV neutrinos (see Ref. [10] for general arguments), for which the Bethe-Heitler suppression is relevant. The pileup and steep tail in cosmic-ray spectra due to their cooling are also considered. Third, we computed electromagnetic cascades, which is essential to test the scenario for IceCube neutrinos. Our model does not need the assumption on primary electrons.

[1] M. Aartsen *et al.* (IceCube Collaboration), Phys. Rev. Lett. **111**, 021103 (2013).

[2] M. Aartsen *et al.* (IceCube Collaboration), Science **342**, 1242856 (2013).

[3] M. Aartsen *et al.* (IceCube Collaboration), Phys. Rev. D **91**, 022001 (2015).

[4] M. G. Aartsen *et al.* (IceCube Collaboration), Astrophys. J. **809**, 98 (2015).

[5] M. Aartsen *et al.* (IceCube Collaboration), arXiv:2001.09520.

[6] J. F. Beacom and J. Candia, J. Cosmol. Astropart. Phys. 11 (2004) 009.

[7] R. Laha, J. F. Beacom, B. Dasgupta, S. Horiuchi, and K. Murase, Phys. Rev. D **88**, 043009 (2013).

[8] M. G. Aartsen *et al.* (IceCube Collaboration), Astrophys. J. **833**, 3 (2016).

[9] W. C. Haack *et al.*, Proc. Sci., ICRC2017 (**2017**) 1005, https://pos.sissa.it/301/.

[10] K. Murase, D. Guetta, and M. Ahlers, Phys. Rev. Lett. **116**, 071101 (2016).

[11] K. Murase and M. Fukugita, Phys. Rev. D **99**, 063012 (2019).

[12] A. C. Fabian and X. Barcons, Annu. Rev. Astron. Astrophys. **30**, 429 (1992).

[13] Y. Ueda, M. Akiyama, K. Ohta, and T. Miyaji, Astrophys. J. **598**, 886 (2003).

[14] G. Hasinger, T. Miyaji, and M. Schmidt, Astron. Astrophys. **441**, 417 (2005).

[15] M. Ajello *et al.*, Astrophys. J. **689**, 666 (2008).

[16] Y. Ueda, M. Akiyama, G. Hasinger, T. Miyaji, and M. G. Watson, Astrophys. J. **786**, 104 (2014).

[17] L. Costamante, Int. J. Mod. Phys. D **22**, 1330025 (2013).

[18] Y. Inoue, in *5th International Fermi Symposium Nagoya, Japan, 2014* (2014).

[19] M. Fornasa and M. A. Sánchez-Conde, Phys. Rep. **598**, 1 (2015).

[20] Y. Inoue, T. Totani, and Y. Ueda, Astrophys. J. **672**, L5 (2008).

[21] M. Ajello *et al.*, Astrophys. J. **699**, 603 (2009).

[22] A. Lien and B. D. Fields, Astrophys. J. **747**, 120 (2012).

[23] D. Eichler, Astrophys. J. **232**, 106 (1979).

[24] V. S. Berezinskii and V. L. Ginzburg, Mon. Not. R. Astron. Soc. **194**, 3 (1981).

[25] M. C. Begelman, B. Rudak, and M. Sikora, Astrophys. J. **362**, 38 (1990).

[26] F. W. Stecker, C. Done, M. H. Salamon, and P. Sommers, Phys. Rev. Lett. **66**, 2697 (1991).

[27] D. Kazanas and D. C. Ellison, Astrophys. J. **304**, 178 (1986).

[28] A. A. Zdziarski, Astrophys. J. **305**, 45 (1986).

[29] M. Sikora, J. G. Kirk, M. C. Begelman, and P. Schneider, Astrophys. J. **320**, L81 (1987).

[30] G. M. Madejski *et al.*, Astrophys. J. **438**, 672 (1995).

[31] C. Ricci *et al.*, Mon. Not. R. Astron. Soc. **480**, 1819 (2018).

[32] S. L. Shapiro, A. P. Lightman, and D. M. Eardley, Astrophys. J. **204**, 187 (1976).

[33] R. A. Sunyaev and L. G. Titarchuk, Astron. Astrophys. **86**, 121 (1980), https://ui.adsabs.harvard.edu/abs/1980A%26A....86..121S/abstract.

[34] A. A. Zdziarski, W. N. Johnson, and P. Magdziarz, Mon. Not. R. Astron. Soc. **283**, 193 (1996).

[35] J. Poutanen and R. Svensson, Astrophys. J. **470**, 249 (1996).

[36] F. Haardt, L. Maraschi, and G. Ghisellini, Astrophys. J. **476**, 620 (1997).

[37] E. P. T. Liang and R. H. Price, Astrophys. J. **218**, 247 (1977).

[38] A. A. Galeev, R. Rosner, and G. S. Vaiana, Astrophys. J. **229**, 318 (1979).

[39] S. A. Balbus and J. F. Hawley, Astrophys. J. **376**, 214 (1991).

[40] S. A. Balbus and J. F. Hawley, Rev. Mod. Phys. **70**, 1 (1998).

[41] K. A. Miller and J. M. Stone, Astrophys. J. **534**, 398 (2000).

[42] A. Merloni and A. C. Fabian, Mon. Not. R. Astron. Soc. **321**, 549 (2001).

[43] B. F. Liu, S. Mineshige, F. Meyer, E. Meyer-Hofmeister, and T. Kawaguchi, Astrophys. J. **575**, 117 (2002).

[44] E. G. Blackman and M. E. Pessah, Astrophys. J. **704**, L113 (2009).

[45] Y. Io and T. K. Suzuki, Astrophys. J. **780**, 46 (2014).

[46] T. K. Suzuki and S.-i. Inutsuka, Astrophys. J. **784**, 121 (2014).

[47] Y.-F. Jiang, J. M. Stone, and S. W. Davis, Astrophys. J. **784**, 169 (2014).

[48] A. Lazarian, L. Vlahos, G. Kowal, H. Yan, A. Beresnyak, and E. M. de Gouveia Dal Pino, Space Sci. Rev. **173**, 557 (2012).

[49] R. Narayan and I.-s. Yi, Astrophys. J. **428**, L13 (1994).

[50] F. Yuan and R. Narayan, Annu. Rev. Astron. Astrophys. **52**, 529 (2014).

[51] F. Takahara and M. Kusunose, Prog. Theor. Phys. **73**, 1390 (1985).

[52] R. Mahadevan, R. Narayan, and J. Krolik, Astrophys. J. **486**, 268 (1997).

[53] R. Mahadevan and E. Quataert, Astrophys. J. **490**, 605 (1997).

[54] S. S. Kimura, K. Toma, and F. Takahara, Astrophys. J. **791**, 100 (2014).

[55] J. W. Lynn, E. Quataert, B. D. G. Chandran, and I. J. Parrish, Astrophys. J. **791**, 71 (2014).

[56] D. Ball, F. Ozel, D. Psaltis, C.-K. Chan, and L. Sironi, Astrophys. J. **853**, 184 (2018).

[57] S. S. Kimura, K. Toma, T. K. Suzuki, and S.-i. Inutsuka, Astrophys. J. **822**, 88 (2016).

[58] S. S. Kimura, K. Tomida, and K. Murase, Mon. Not. R. Astron. Soc. **485**, 163 (2019).

[59] In this work, CRs are used for nonthermal ions and nucleons that do not have to be observed on Earth.

[60] F. Panessa, R. D. Baldi, A. Laor, P. Padovani, E. Behar, and I. McHardy, Nat. Astron. **3**, 387 (2019).

[61] H. Netzer, Annu. Rev. Astron. Astrophys. **53**, 365 (2015).

[62] A. Koratkar and O. Blaes, Publ. Astron. Soc. Pac. **111**, 1 (1999).

[63] N. I. Shakura and R. A. Sunyaev, Astron. Astrophys. **24**, 337 (1973), https://ui.adsabs.harvard.edu/abs/1973A%26A....24..337S/abstract.

[64] L. C. Ho, Annu. Rev. Astron. Astrophys. **46**, 475 (2008).

[65] B. Trakhtenbrot *et al.*, Mon. Not. R. Astron. Soc. **470**, 800 (2017).

[66] P. F. Hopkins, G. T. Richards, and L. Hernquist, Astrophys. J. **654**, 731 (2007).

[67] J. A. Mayers *et al.*, arXiv:1803.06891.

[68] See Supplemental Material at http://link.aps.org/supplemental/10.1103/PhysRevLett.125.011101 for technical details about the modeling of disk-corona spectra, timescales for protons and electron-positron pairs, calculations of nonthermal proton spectra and the resulting extragalactic neutrino background, and the detectability of nearby AGN.

[69] J. Pringle, Annu. Rev. Astron. Astrophys. **19**, 137 (1981).

[70] S. Kato, J. Fukue, and S. Mineshige, *Black-Hole Accretion Disks—Towards a New Paradigm—, 549 pages, including 12 Chapters, 9 Appendixes*, ISBN 978-4-87698-740-5 (Kyoto University Press, Japan, 2008) (Kyoto University Press, 2008).

[71] T. Di Matteo, E. G. Blackman, and A. C. Fabian, Mon. Not. R. Astron. Soc. **291**, L23 (1997).

[72] X. Cao, Mon. Not. R. Astron. Soc. **394**, 207 (2009).

[73] C. Jin, M. Ward, C. Done, and J. Gelbord, Mon. Not. R. Astron. Soc. **420**, 1825 (2012).

[74] C. W. Morgan *et al.*, Astrophys. J. **756**, 52 (2012).

[75] P. A. Becker, T. Le, and C. D. Dermer, Astrophys. J. **647,** 539 (2006).

[76] L. Stawarz and V. Petrosian, Astrophys. J. **681,** 1725 (2008).

[77] J. S. Chang and G. Cooper, J. Comput. Phys. **6,** 1 (1970).

[78] B. T. Park and V. Petrosian, Astrophys. J. Suppl. Ser. **103,** 255 (1996).

[79] S. S. Kimura, K. Murase, and P. Mészáros, Phys. Rev. D **100,** 083014 (2019).

[80] C. D. Dermer, J. A. Miller, and H. Li, Astrophys. J. **456,** 106 (1996).

[81] C. D. Dermer, K. Murase, and Y. Inoue, J. High Energy Astrophys. **3–4,** 29 (2014).

[82] M. Hoshino, Phys. Rev. Lett. **114,** 061101 (2015).

[83] X. Li, F. Guo, H. Li, and G. Li, Astrophys. J. **811,** L24 (2015).

[84] F. Ozel, D. Psaltis, and R. Narayan, Astrophys. J. **541,** 234 (2000).

[85] S. S. Kimura, K. Murase, and K. Toma, Astrophys. J. **806,** 159 (2015).

[86] D. Ball, F. Ozel, D. Psaltis, and C.-k. Chan, Astrophys. J. **826,** 77 (2016).

[87] K. Murase, Phys. Rev. D **97,** 081301(R) (2018).

[88] K. Murase, A. Franckowiak, K. Maeda, R. Margutti, and J. F. Beacom, Astrophys. J. **874,** 80 (2019).

[89] M. J. Chodorowski, A. A. Zdziarski, and M. Sikora, Astrophys. J. **400,** 181 (1992).

[90] S. Stepney and P. W. Guilbert, Mon. Not. R. Astron. Soc. **204,** 1269 (1983).

[91] K. Murase and J. F. Beacom, Phys. Rev. D **82,** 043008 (2010).

[92] K. Murase, Y. Inoue, and C. D. Dermer, Phys. Rev. D **90,** 023007 (2014).

[93] M. Ajello et al., Astrophys. J. **800,** L27 (2015).

[94] K. Murase, S. Inoue, and S. Nagataki, Astrophys. J. **689,** L105 (2008).

[95] K. Kotera, D. Allard, K. Murase, J. Aoi, Y. Dubois, T. Pierog, and S. Nagataki, Astrophys. J. **707,** 370 (2009).

[96] K. Fang and K. Murase, Nat. Phys. Lett. **14,** 396 (2018).

[97] Y. Inoue, Astrophys. J. **733,** 66 (2011).

[98] C.-Y. Chen, P. S. Bhupal Dev, and A. Soni, Phys. Rev. D **92,** 073001 (2015).

[99] A. Palladino and W. Winter, Astron. Astrophys. **615,** A168 (2018).

[100] Y. Fukada, S. Hayakawa, I. Kasahara, F. Makino, Y. Tanaka, and B. V. Sreekantan, Nature (London) **254,** 398 (1975).

[101] K. Watanabe, D. H. Hartmann, M. D. Leising, L. S. The, G. H. Share, and R. L. Kinzer, in Proceedings of the Fourth Compton Symposium, American Institute of Physics Conference Series, Vol. 410, edited by C. D. Dermer, M. S. Strickman, and J. D. Kurfess (1997), pp. 1223–1227, https://dx.doi.org/10.1063/1.53933.

[102] G. Weidenspointner, M. Varendorff, S. C. Kappadath, K. Bennett, H. Bloemen, R. Diehl, W. Hermsen, G. G. Lichti, J. Ryan, and V. Schönfelder, in American Institute of Physics Conference Series, Vol. 510, edited by M. L. McConnell and J. M. Ryan (2000), pp. 467–470, https://dx.doi.org/10.1063/1.1307028.

[103] M. Ackermann et al. (Fermi LAT Collaboration), Astrophys. J. **799,** 86 (2015).

[104] K. Murase, K. Ioka, S. Nagataki, and T. Nakamura, Phys. Rev. D **78,** 023005 (2008).

[105] F. W. Stecker, Phys. Rev. D **88,** 047301 (2013).

[106] O. Kalashev, D. Semikoz, and I. Tkachev, J. Exp. Theor. Phys. **120,** 541 (2015).

[107] E. Waxman and J. N. Bahcall, Phys. Rev. D **59,** 023002 (1998).

[108] K. Murase and E. Waxman, Phys. Rev. D **94,** 103006 (2016).

[109] K. Murase, K. Asano, T. Terasawa, and P. Meszaros, Astrophys. J. **746,** 164 (2012).

[110] G. G. Howes, J. M. Ten Barge, W. Dorland, E. Quataert, A. A. Schekochihin, R. Numata, and T. Tatsuno, Phys. Rev. Lett. **107,** 035004 (2011).

[111] M. Aartsen et al. (IceCube Collaboration), Phys. Rev. Lett. **124,** 051103 (2020).

[112] A. Lamastra, F. Fiore, D. Guetta, L. A. Antonelli, S. Colafrancesco, N. Menci, S. Puccetti, A. Stamerra, and L. Zappacosta, Astron. Astrophys. **596,** A68 (2016).

[113] A. De Angelis et al. (e-ASTROGAM Collaboration), Exp. Astron. **44,** 25 (2017).

[114] A. Moiseev et al., Proc. Sci., ICRC2017 (**2017**) 798, https://pos.sissa.it/301/.

[115] T. Aramaki, P. Hansson Adrian, G. Karagiorgi, and H. Odaka, Astropart. Phys. **114,** 107 (2020).

[116] M. G. Aartsen et al. (IceCube Collaboration), Eur. Phys. J. C **79,** 234 (2019).

[117] M. Aartsen et al. (IceCube-Gen2 Collaboration), arXiv:1412.5106.

[118] S. Adrian-Martinez et al. (KM3Net Collaboration), J. Phys. G **43,** 084001 (2016).

[119] Y. Inoue, K. Murase, G. M. Madejski, and Y. Uchiyama, Astrophys. J. **776,** 33 (2013).

[120] A. P. Szabo and R. J. Protheroe, Astropart. Phys. **2,** 375 (1994).

[121] F. W. Stecker and M. H. Salamon, Space Sci. Rev. **75,** 341 (1996).

[122] J. Alvarez-Muniz and P. Mészáros, Phys. Rev. D **70,** 123001 (2004).

[123] Y. Inoue and A. Doi, Publ. Astron. Soc. Jpn. **66,** L8 (2014).

[124] Y. Inoue and A. Doi, Astrophys. J. **869,** 114 (2018).

[125] Y. Inoue, D. Khangulyan, S. Inoue, and A. Doi, arXiv:1904.00554.